

Multiwavelength simultaneous observation of Blazar 3C454.3 at the gamma rays flare in November 2007

Y.A.Mori¹, J.Kataoka¹, N.Kawai¹, MITSuME/Suzaku/AGILE team

¹ Tokyo Institute of Technology, Meguro, Tokyo, Japan
E-mail(YAM): ymori@hp.phys.titech.ac.jp

ABSTRACT

The spectrum of blazars span over 20 decades from radio to gamma rays. To clarify a variety of physical phenomena of the blazar jets, a blazar must be monitored *in multiwavelengths* and *simultaneously*.

We succeeded in simultaneous multiwavelength observation of a blazar 3C 454.3, a QHB (quasar-hosted blazar) at $z=0.859$. It also belongs to the brightest quasar class, with its luminosity reaching 10^{48} erg/s. A huge gamma-ray flare of 3C 454.3 was reported by the AGILE satellite on November 2nd through December 1st, 2007. We proposed a ToO observation with the Suzaku satellite, which was approved and performed on Dec 5, 6. At the same time, we were monitoring its optical magnitudes in three colors (g' , R_c , I_c) using the MITSuME Telescope at the ICRR Akeno Observatory, Yamanashi, Japan. Its R band magnitude increased from $R=16$ up to $R=13.4$ on December 1. We present the spectral energy distribution based on this multiwavelength observation, and discuss the emission models.

KEY WORDS: quasars:individual:3C 454.3 — X rays: Suzaku — optical: MITSuME

1. Introduction

1.1. Active Galactic Nuclei

Active galactic nucleus (AGN) is a compact luminous region at the center of a galaxy. The outstanding properties of AGNs are: high luminosity $> 10^{44}$ erg/s, sometimes reaches to 10^{49} erg/s, nonthermal emission in the radio, infrared, optical, ultra-violet, X-ray and gamma ray wavebands, rapid variability as short as hours. About 10 % of AGN has significant outflows named 'jet' from the supermassive black hole at the center of the host galaxy.

1.2. Blazar

Blazar is a class of AGN, which direction from observer $\theta \sim 1/\Gamma_{BLK} \sim 5$ degree. This narrow θ is occurred relativistic beaming effect. Its Spectral Energy Distribution (SED) has double-humped shape by Synchrotron Radiation in low energy side and Inverse Compton scattering in high energy side.

Blazar has a characteristic called Blazar Sequence, which negative relation of peak energy of hump and frequency of peak energy (see Fig.1). Blazar is divided into three classes by Blazar Sequence. From High frequency of peak energy these are named 'High-frequency peak BL Lac (HBL)', 'Low-frequency peak BL Lac (LBL)', 'Quasar Hosted Blazar (QHB)'. SED of QHB shows the peak energy of Inverse Compton scattering is larger than

one of Synchrotron Radiation hump, so QHB needs External Compton scattering.

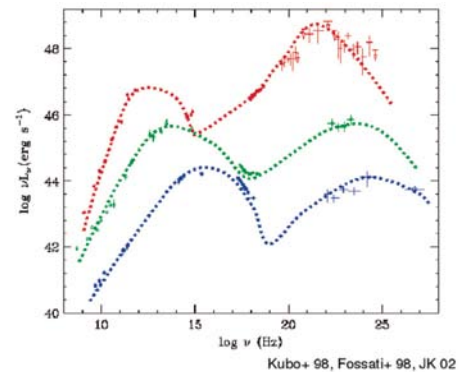


Fig. 1. SED of three classes of Blazar Sequence : The blue line shows High-frequency peak BL Lac (HBL), the green line shows Low-frequency peak BL Lac (LBL), the red line shows Quasar Hosted Blazar (QHB). The peak energy of hump has negative relation to the frequency of peak energy.

1.3. 3C 454.3

Among the Quasar Hosted Blazar (QHB) class of blazars, 3C454.3 ($z = 0.859$, R.A. = 22:53:57.7, Dec. = +16:08:54) is one of the brightest sources. QHB shows all the typical hallmarks of the class of blazar: large intensity variations at all frequencies, high radio and opti-

cal polarization, superluminal motion and a SED showing two broad peaks attributed to Synchrotron Radiation and Inverse Compton scattering. The Synchrotron power peaks in the Infra-red band while Inverse Compton scattering starts at soft X-ray frequencies and peaks at MeV energies (Giommi et al. 2002; Blom et al.1995)

In November-December 2007, 3C454.3 exploded and reach at optical 13.4 mag. This event triggered observations at gamma-ray energies with AGILE satellite. The Suzaku satellite pointed 3C454.3 as a Target of Opportunity (ToO) in X-ray band on Dec 5,6. The optical observations performed with the ground-based MITSuME telescope.

2. MITSuME telescope Instrument

Multicolor Imaging Telescopes for Survey and Monstrous Explosions (MITSuME) are a robotic telescope located at ICRR Akeno Observatory, Yamanashi, Japan and OAO, Okayama, Japan. The each MITSuME telescope has a Tricolor Camera, which allows us to take simultaneous images in g', Rc and Ic bands. This Camera have a 28 x 28 arcmin field of view.

These telescopes are built to perform for optical afterglow of Gamma-Ray Bursts (GRB), and respond to GRB Coordinate Network (GCN) alerts and start taking tricolor images automatically.

When there is no GRB that can be observed, MITSuME Akeno telescope observe about 10 AGNs everyday, and create light curve to monitor activity of the flare.



Fig. 2. MITSuME Akeno 50cm

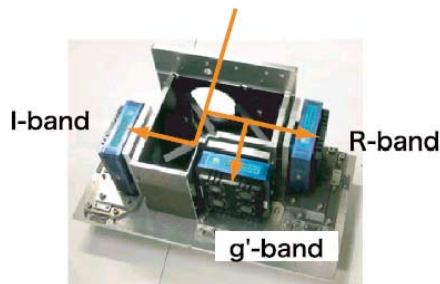


Fig. 3. Tricolor Camera

3. Observation of 3C 454.3

3.1. MITSuME observation

MITSuME Akeno Telescope observed 3C 454.3 several times in November and December, we analyzed data about two weeks, its include the data when simultaneous with Suzaku, i.e.that performed on December 5.

All raw g',R,I frames obtained by MITSuME were corrected for dark, bias and flat field with IRAF v 2.12. Instrumental magnitudes were obtained via aperture photometry using DAOPHOT (Stetson 1998) and Sextractor (Bertin & Arnouts 1996). Calibration of the optical source magnitude was obtained by differential photometry with respect to the comparison stars sequence reported by Raiteri et al. (1998) and Gonzalez-Perez et al. (2001). The fluxes are corrected for the Galactic extinction corresponding to a reddening of $E\{B-V\} = 0.108$ mag (Schlegel et al.1998).

At the same time, the Rapid Eye Mount (REM, Zerbi et al. 2004) telescope also observed 3C 454.3 on November and December, and data were analyzed by REM team.

The light curve in the R band of MITSuME and REM are shown in Fig.4.

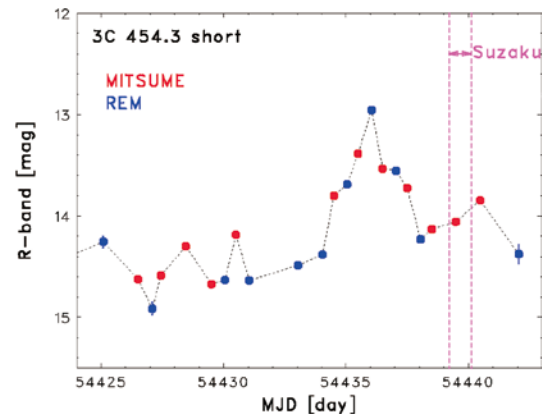


Fig. 4. MITSuME and REM light curve of 3C 454.3 in the R band from November 20 to December 8 : The red points and blue points show MITSuME and REM data (Tosti et al. in prep) respectively. The dates of Suzaku pointed observations of Dec 5, 6 are indicated by the dashed vertical lines.

3.2. Suzaku observation

3C 454.3 was observed by Suzaku between December 5-6. The total exposure time is 40 ksec. Event files from version 2.1.6.16 of the Suzaku pipeline processing were used and spectrum were extracted using XSELECT.

For each XIS, source spectra were extracted from circular regions of 4.3 arcmin radius centered on the source.

Fig. 5 shows the 0.4 - 2 keV, 2 - 10 keV XIS light curve and the hardness ratio from the Suzaku observation of 3C 454.3. The light curve of Suzaku data has about 10 %

time variance, and the hardness ratio is almost constant. So the spectrum were made from total accumulated data.

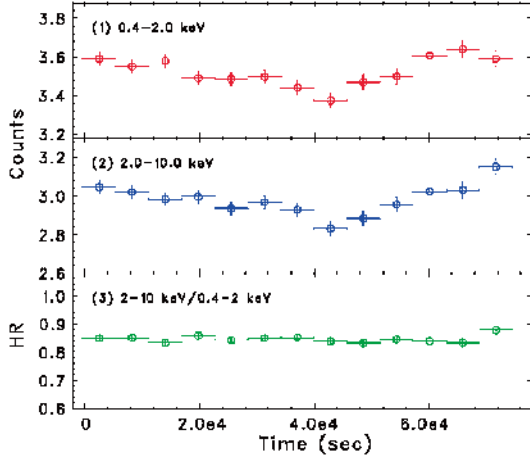


Fig. 5. Suzaku light curve of 3C 454.3 on December 5-6 : Panels from top to bottom show the 0.4 - 2 keV, 2 - 10 keV light curve, the hardness ratio (0.4 - 2 keV / 2 - 10 keV) respectively. The time variance is about 10 %, and the hardness ratio is constant.

All spectral fits were performed using XSPEC version 11.3.2ag. Errors on model parameters are quoted at the 90 percent confidence level. We applied a simple power law with Galactic absorption model according to $N_H = 0.724 \times 10^{21} \text{ cm}^{-2}$ (Kalberla et al 2005). We obtained the photon index is $\Gamma = 1.51 \pm 0.003$.

The spectrum fitted with the above model are displayed in the top panels of Fig.6. The bottom panel shows the ratio between the data and the folded model. We note large deviation between the data and the model at low energy.

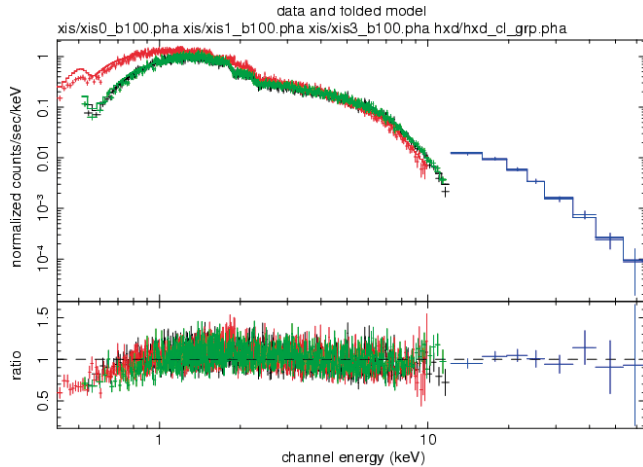


Fig. 6. Suzaku spectrum of 3C 454.3 on December 5-6 : High-precision X-ray spectrum from 0.4 to 60 keV. black points, red points, green points, blue points represent XIS0, XIS1, XIS3, HXD data, respectively. The bottom panel shows the ratio between the data and the folded model, a power law with Galactic absorption.

4. Broad-band spectral energy distribution

We combined our MITSuME, Suzaku measurements with non-simultaneous multifrequency data from NED to build the SED shown in Fig.7 and Fig.8. The general shape of the SED clearly follows the usual two-bump Synchrotron / Inverse Compton scenario.

First, we tried to fit the SED data with one-zone Synchrotron + Synchrotron self-Compton (SSC) models from a power law distribution of relativistic electrons with Lorentz factor of $\gamma_{min} = 1$, $\gamma_p = 200$ and $\gamma_{max} = 6000$ (see Fig.8). We found that this model can not explain the high energy at high frequency ($> 10^{22}$ Hz) . Moreover, this model does not fit to cut-off around 1 keV. (see Fig.7)

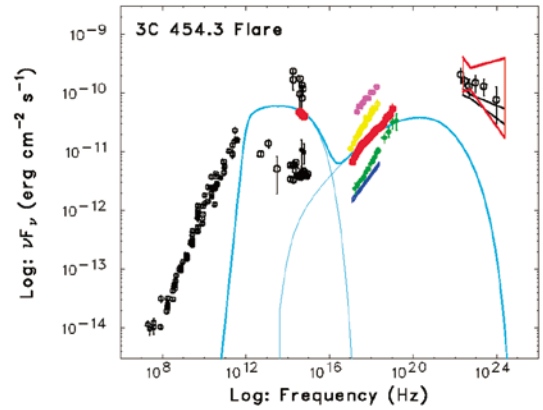


Fig. 7. SED of 3C454.3 : The sky blue line is Synchrotron + Synchrotron Self Compton model. The red points represent MIT-SuME, Suzaku, AGILE data (preliminary; Vercellone et al. in prep) on December 5-6. The black points represent from NED. The pink, yellow, green, blue represent previous observation by X-ray satellites

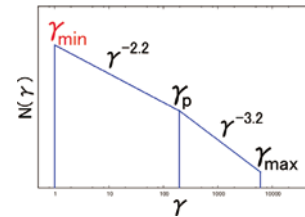


Fig. 8. electron distribution : the γ_{min} is lower limit of electron distribution. the γ_{max} is higher limit of one.

Next, we tried to fit the SED data with Synchrotron + External Compton (ERC) models from a power law distribution of relativistic electrons with Lorentz factor of $\gamma_{min} = 1$, $\gamma_p = 200$ and $\gamma_{max} = 6000$ (see Fig.8). We obtained reasonably good representations of the data for both the high energy at high frequency, and cut-off around 1 keV assuming parameters in Table.1. (see Fig.9)

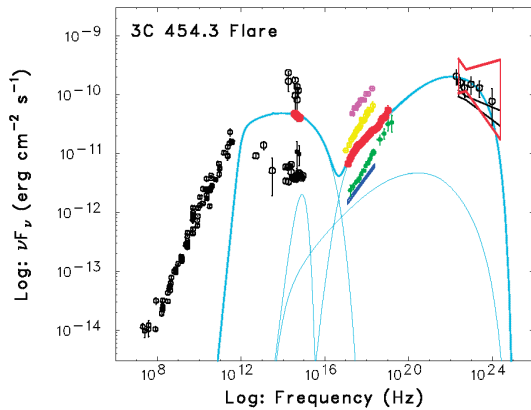


Fig. 9. SED of 3C454.3 : blue line is Synchrotron + External Compton scattering model. red points represent MITSuME, Suzaku, AGILE data on December 5-6. The black points represent from NED. The pink, yellow, green, blue represent previous observation by X-ray satellites

Table 1. parameters of Synchrotron + ERC model

electron distribution	
γ_{min}	1
γ_p	200
γ_{max}	6000
power1	2.2 ($\gamma_{min} < \gamma < \gamma_p$)
power2	3.2 ($\gamma_p < \gamma < \gamma_{max}$)
jet	
Γ	10
Θ	0.1 rad
B	10 Gauss
T_{disk}	1.0e4 K
L_{BLR}	1.35e43 erg/s
L_{sync}	1.30e43 erg/s
L_{SSC}	1.60e47 erg/s
L_{ERC}	5.8e48 erg/s
L_{elec}	1.1e45 erg/s
U_e/U_B	1/30

We tried to fit the SED data with ERC models case of $\gamma_{min} = 2$, and $\gamma_{min} = 3$. (see Fig.10) The result of fitting indicates that only $\gamma_{min} = 1$ is accepted to reproduce the data.

5. Conclusion

We succeeded in simultaneous multi-wavelength observations of a blazar 3C 454.3 at the “gamma-ray flare” for the first time. There is a remarkable cut-off at X ray spectrum. Its precise measurement of the low-energy limit of accelerated electrons $\gamma_{min} = 1$.

Multiwavelength spectrum is well fitted by ERC

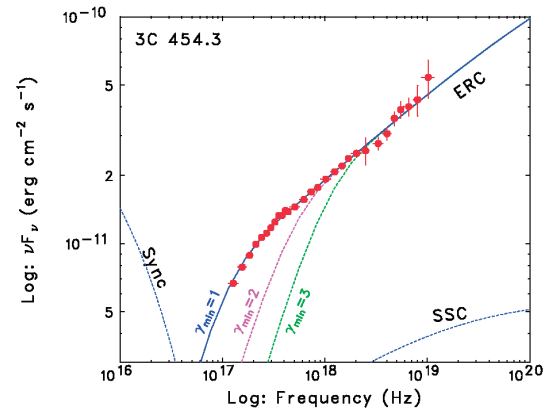


Fig. 10. An enlargement SED at around 1 keV : blue line, pink line, green line is Synchrotron + ERC model when $\gamma_{min} = 1, 2, 3$ respectively.

model. The γ rays are due to the Compton scattering of seed photons if $T \sim 10^{4-5}$ K.

6. Multiwavelength observation with Fermi Gamma-Ray Space Telescope / MAXI

We plan multi-wavelength observation of 8 AGNs after Fermi Gamma-Ray Space Telescope launched (see Table.2). We expect to conduct non-bias blazar survey even when the source is in a low state (see Fig.11).

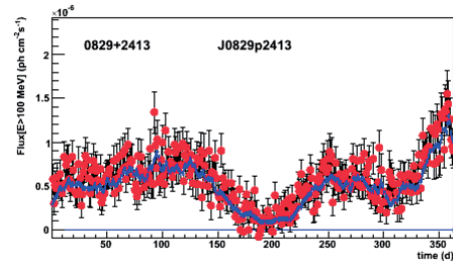


Fig. 11. Simulation of Fermi Gamma-Ray Space Telescope : Simulated Fermi Gamma-Ray Space Telescope light curve of Q0827+243 for 1 day binning of data.

acknowledgments. We would appreciate all member of MITSuME, Suzaku, AGILE team.

References

- Blom et al.1995, A&A, 295, 330
- Fossati, G. et al. 1998 MNRAS., 299, 433F
- Ghisellini, G. et al. 2007 MNRAS., 382L, 82G
- Giommi, P. et al. 2002 babs.conf, 63G
- Gonzalez-Perez et al. 2001 AJ, 122, 2055G
- Kubo, H. et al. 1998 ApJ., 504, 693K
- Raiteri, C. M. et al. 2007 A&A., 473, 819R
- Raiteri, C. M. et al. 1998 A&AS., 130, 495R
- Schlegel, D.J. et al.1998 ApJ., 500, 525
- Zerbi, F. et al. 2004 SPIE, 5492, 1590

Table 2. Source list of multiwavelength observation with Fermi Gamma-Ray Space Telescope

Source Name	z	class	Flux (2-10 keV) [10^{-12} erg/cm ² /s]	Flux (> 100 MeV) [10^{-5} ph/cm ² /s]
PKS 0208-512	1	HPQ	9.5	85.5 ± 4.5
Q0827+243	0.94	LPQ	4.8	24.9 ± 3.9
PKS 1127-145	1.184	LPQ	11	38.3 ± 8.0
PKS 1510-089	0.36	LPQ	10	18.0 ± 3.8
3C 454.3	0.86	HPQ	11	53.7 ± 4.0
3C 279	0.536	HPQ	13	89 ± 3.2
PKS 0528+134	2.06	LPQ	30	60 ± 3.0
PKS 2126-15	3.3	LPQ	12	